

COMMISSION INTERNATIONALE
DES GRANDES BARRAGES

VINGT SEPTIÈME CONGRÈS
DES GRANDES BARRAGES
MARSEILLE, JUIN 2022

**SEISMIC PERFORMANCE VERIFICATION OF A ROCKFILL DAM AGAINST
LARGE DOUBLET EARTHQUAKES (*)**

Nario YASUDA
Head of Eng. Division 1,
JAPAN DAM ENGINEERING CENTER

Zengyan CAO
Senior Engineer,
J-POWER BUSINESS SERVICE CORPORATION,

JAPAN

SUMMARY

The purpose of this study is to clarify the behavior of a rockfill dam during large doublet earthquakes and to propose a procedure for verifying the seismic performance of rockfill dams during such earthquakes. Impacted by a strong earthquake, the dynamic characteristics of the Aratozawa Dam significantly changed temporarily. The behavior of the dam subject to another strong earthquake before its dynamic characteristics had recovered was predicted. Based on the analysis results, the seismic performance of the dam was evaluated. The results clarified that the change in the dynamic characteristics of the dam in response to the first event greatly affected the behavior of the dam during the second event. In addition, a method was proposed for predicting the final residual subsidence of the dam by summing the sliding displacement caused by each earthquake and the subsidence related to the shaking and rearrangement of soil particles. It is recommended that after a dam experiences a strong earthquake, the reservoir is adjusted to a safe water level and maintained at that level for a minimum of one week as an emergency response measure.

* *Vérification des performances sismiques d'un barrage en enrochement contre des doublets de séismes*

RÉSUMÉ

Le but de ce rapport est de clarifier le comportement d'un barrage en enrochement lors de doublet de grands tremblements de terre et de proposer une procédure de vérification des performances sismiques des barrages en enrochement lors de tels séismes. Impactées par le tremblement de terre d'Iwate-Miyagi Nairiku en 2008, les caractéristiques dynamiques du barrage d'Aratozawa ont changé temporairement de manière significative. Le comportement du barrage soumis à un autre puissant tremblement de terre avant que ses caractéristiques dynamiques se soient rétablies a été prévu. Sur la base des résultats de l'analyse, la performance sismique du barrage a été évaluée. Les résultats expliquent que le changement des caractéristiques dynamiques du barrage en réponse au premier événement a grandement affecté le comportement dynamique du barrage lors du deuxième événement. De plus, une méthode a été proposée afin de prévoir l'affaissement résiduel final du barrage en additionnant le déplacement glissant provoqué par chaque séisme et l'affaissement lié aux secousses et au réarrangement des particules du sol. Il est recommandé, après qu'un barrage ait subi un fort tremblement de terre, que le réservoir soit ajusté à un niveau d'eau sécurisé et maintenu à ce niveau pendant au moins une semaine comme mesure d'intervention d'urgence.

1. INTRODUCTION

In Japan, seismic performance verification of existing dams against large earthquakes is being carried out via dynamic response analysis. In the dynamic response analysis of these dams, engineers use the dam's normal operating conditions as the initial conditions for the analyses and suppose the dam subject to a single earthquake. However, after the Iwate-Miyagi Nairiku Earthquake in 2008 (M_j 7.2, where M_j is the Japan Meteorological Agency (JMA) magnitude scale), the dynamic characteristics of the Aratozawa Dam, a 74.4 m high rockfill dam, considerably deteriorated [1][2]. Approximately one week after the main shock, the natural frequencies of the dam were found to have nearly recovered. On the other hand, during the 2016 Kumamoto earthquake of April 14 (21:26, Japan time) and 16 (01:25), (M_j 6.5 and M_j 7.3), Mashiki Town experienced ground motions of JMA seismic intensity 7 twice within 28 hours [3]. Generally, large aftershocks often occur after a strong inland earthquake. In the future, a dam may experience multiple large seismic events in a short period. Thus, it is necessary and beneficial to dam engineering to investigate the behavior of the Aratozawa Dam subject to a ground motion of JMA seismic intensity 7 before its dynamic characteristics fully recover from an earlier earthquake. The situation mentioned here has not been addressed in the current "Guidelines of the Seismic Performance Verification of Dams for Large-scale Earthquakes (draft)" [4]. Thus, this study clarifies the behavior of rockfill dams subject to large doublet earthquakes and proposes a seismic performance verification method and emergency

response measures in preparation for the occurrence of large doublet earthquakes in the future.

In this study, the authors modeled the response of the Aratozawa Dam to two large earthquakes. The dynamic response analyses of the dam are performed considering the variation in the dynamic characteristics of the dam during each earthquake. The calculations of slip deformation and the deformation related to the shaking and rearrangement of soil particles are carried out considering the change in the material properties of the dam. The final residual deformation of the dam after the doublet earthquakes is predicted by summing the deformation induced by each earthquake, and the seismic safety of the dam is verified via the residual deformation. In addition, in preparation for large doublet earthquakes, emergency response measures after large earthquakes are investigated for rockfill dams.

2. DAM SPECIFICATIONS AND EARTHQUAKE MONITORING

2.1. DAM SPECIFICATIONS

The Aratozawa Dam is a 74.4 m high rockfill dam with a central clay core on the Kitakami River, Kurihara City, Miyagi Prefecture, and the dam body was completed in 1992. Table 1 shows the specifications of the dam. The location, the plan view and the standard cross-section of the dam and the locations of seismographs are shown in Fig. 1. The seismographs with three components (parallel and perpendicular to the dam axis and vertical directions) are installed at the dam base (F), mid-height of the core (M) and dam crest (T).

Table 1
Specifications of the Aratozawa Dam.

Dam location	Kurihara City, Kurihara district, Miyagi Prefecture
Dam type	Rockfill dam with central clay core
Dam height	74.4 m (minimum ground elevation, EL. 205.0 m)
Crest length	413.7 m
Crest width	10.0 m
Crest elevation	EL. 279.4 m
Nonoverflow section elevation	EL. 278.9 m
Slope gradient	Upstream: 1: 2.7 downstream: 1: 2.1
Embankment volume	3048000 m ³
Basin area	20.4 km ²
Reservoir storage volume	13850000 m ³
Design seismic coefficient	0.15 (dam body), 0.18 (intake tower), 0.16 (spillway)

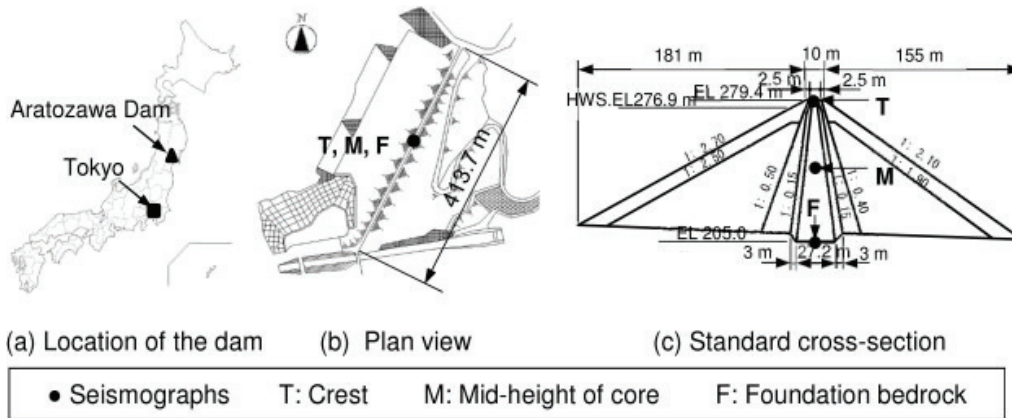


Fig. 1

Location of the dam and the locations of seismographs.
Localisation du barrage et emplacements des sismographes.

2.2. NONLINEAR PROPERTIES OF EMBANKMENT MATERIALS EVALUATED FROM EARTHQUAKE RECORDS

A large number of earthquakes since 1992, immediately after the dam body completion, have been recorded. Of these, there were approximately 500 earthquakes with a maximum acceleration over 10 cm/s^2 and 37 earthquakes over 100 cm/s^2 at the dam base (F). On June 14, 2008, the Iwate-Miyagi Nairiku Earthquake in 2008 (M_j 7.2) occurred. At the Aratozawa Dam located approximately 15 km from the epicenter, the maximum acceleration of 1024 cm/s^2 in the direction perpendicular to the dam axis was recorded at the dam base. This is the largest earthquake magnitude ever recorded at the base of a dam in Japan. During the earthquake, the natural frequency and acceleration amplification factor of the dam sharply decreased. Approximately 1 week after the main shock, the natural frequencies of the dam nearly fully recovered to their preearthquake values.

The decrease in the natural frequency of the dam implies a reduction in the stiffness of the dam materials. In a single degree of freedom system, the relationship of the natural circular frequency ω , the stiffness k and the mass m are expressed as Eq. [1].

$$\omega^2 = \frac{k}{m} \quad (1)$$

The relationship between the three physical quantities in Eq. [1] is also generally satisfied in civil engineering structures such as rockfill dams. Because the mass of the dam body does not change, considering that the stiffness is proportional to the shear modulus G of the dam material through Poisson's ratio, the relationship between the shear modulus G and the fundamental frequency is shown in Eq. [2].

$$\frac{f_1^2}{f_{10}^2} = \frac{G}{G_0} \quad (2)$$

Here, and are the initial shear modulus of the material in the small strain status and the initial fundamental frequency of the dam, respectively. Therefore, the rate of change in the shear modulus of the materials can be obtained from the rate of change in the fundamental frequency of the dam using Eq. [2] [5]. In addition, the transfer function of the dam can be obtained from the earthquake records at the crest of the dam (T) and the dam base (F), and the frequency corresponding to the first peak of the transfer function can be regarded as the fundamental frequency of the dam. From the analysis of the records of the past small earthquakes, the fundamental frequency of the Aratozawa Dam has been found to be 3.2 Hz [2]. To determine the fundamental frequency of the dam for each earthquake, the earthquake records of relatively large acceleration amplitude are extracted, focusing on the Iwate-Miyagi Nairiku Earthquake in 2008 and its aftershocks. The list of the extracted earthquake records is shown in Table 2. These earthquake records (Nos. 1-19) are numbered in the order of occurrence.

Table 2
Earthquake records and the obtained results.

No.	Time of occurrence	M	Focal depth (km)	Max. acc. at the dam base ¹ (cm/s ²)	Fundamental freq. of the dam (Hz)	Average shear strain of dam body
1	1996/08/11 03:12	6.1	9	28	2.930	5.320E-05
2	1996/08/11 08:10	5.8	10	36	2.830	3.920E-05
3	1996/08/11 15:01	4.9	10	30	3.027	6.600E-06
4	2003/05/26 18:24	7.1	72	114	2.637	1.727E-04
5	2008/06/14 08:43	7.2	8	1024	1.514	1.566E-03
6	2008/06/14 09:00	4.2	11	99	2.344	3.700E-06
7	2008/06/14 09:01	4.0	7	482	1.953	7.760E-05
8	2008/06/14 09:14	3.6	4	151	2.246	1.660E-05
9	2008/06/14 09:20	5.7	7	76	2.051	7.980E-05
10	2008/06/14 10:40	4.8	7	120	2.148	5.960E-05
11	2008/06/14 12:09	4.1	8	92	2.246	2.840E-05
12	2008/06/14 12:10	4.8	9	79	2.344	2.480E-05
13	2008/06/14 19:11	4.1	8	229	2.148	5.170E-05
14	2008/06/16 23:14	5.3	7	76	2.246	3.760E-05
15	2008/07/24 00:26	6.8	108	27	2.600	6.530E-05
16	2008/09/25 15:04	4.1	6	119	2.539	7.000E-05
17	2011/03/11 14:46	9.0	24	102	2.307	1.858E-04
18	2011/04/07 23:32	7.2	66	120	2.344	2.405E-04
19	2015/05/1306:13	6.8	46	18	2.942	1.350E-05

Note: ¹The maximum value of the three directional components of the dam base (F).

On the other hand, using the earthquake records of the dam, it is possible to calculate the average shear strain of the dam according to the procedure shown in Fig. 2.

From each earthquake record, the fundamental frequency of the dam in the direction perpendicular to the dam axis and the average shear strain are calculated and summarized in Table 2. The value of G/G_0 is calculated according to Eq. [2] and plotted with the average shear strain γ in Fig 3. Depending on the G/G_0 - γ

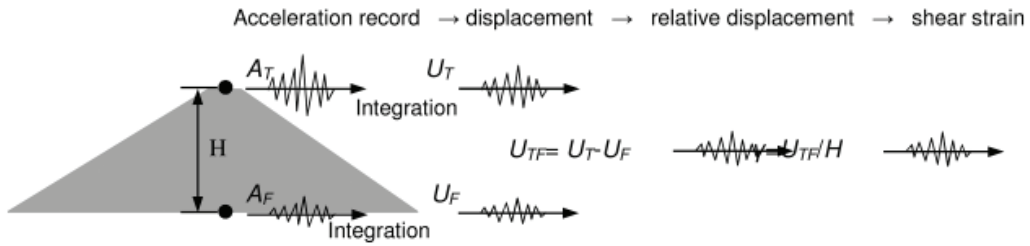


Fig. 2

Procedure for calculating the shear strain of the dam from the recordings.

Procédure de calcul de la déformation de cisaillement du barrage à partir des enregistrements.

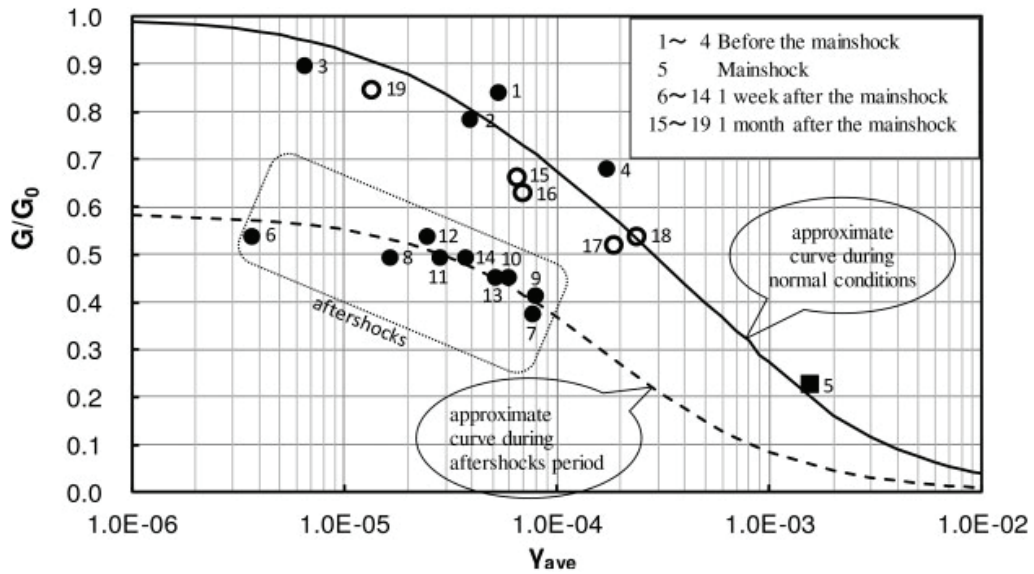


Fig. 3

$G/G_0-\gamma$ relationship obtained from the records of relatively strong earthquakes.
 $G/G_0-\gamma$ relation obtenue à partir des enregistrements de tremblements de terre relativement forts.

relationship and the occurrence time of the earthquakes, this seismicity can be divided into the following 3 periods.

- Period I. Earthquake 1 to earthquake 5
- Period II. Earthquake 6 to earthquake 14
- Period III. Earthquake 15 to earthquake 19

The $G/G_0-\gamma$ relationship in Period I can be approximated by a curve and is clearly different from that in Period II. In response to the Iwate-Miyagi Nairiku Earthquake in 2008 (No. 5), it is clear that the material properties of the Aratozawa Dam had significantly changed temporarily. Thus, during the earthquake response analysis and seismic performance evaluation of the dam in Period II, the dynamic

characteristics and material properties of the dam during this period must be considered. In addition, the G/G_0 - γ relationship in Period III can be estimated to have nearly recovered to the relationship exhibited in Period I. The solid line showing the G/G_0 - γ relationship of the dam in Period I and Period III is very similar to that of ordinary soil materials. The shear strain corresponding to $G/G_0 = 0.5$ is 2.9×10^{-4} , which substantially coincides with the reference shear strain (3.0×10^{-4}) identified by a reproduction analysis of a past earthquake of the Aratozawa Dam [6]. In Period II, there are no data reflecting a shear strain of 10^{-4} or more, but when the existing data are fitted with a hyperbolic line, the relationship indicated by the broken line is obtained.

3. CONSIDERED EVENTS AND STUDY METHODS

3.1. CONSIDERED EVENTS

In this study, it is assumed that the Aratozawa Dam will be subject to a doublet earthquake similar to the 2016 Kumamoto Earthquake. The foreshock (M_j 6.5) of the 2016 Kumamoto Earthquake occurred on April 14, and the main shock (M_j 7.3) occurred on April 16 of the same year. Mashiki Town, Kumamoto Prefecture, experienced the ground motion of JMA seismic intensity 7 (the maximum seismic intensity ever observed in Japan) twice within 28 hours. In this study, the terms “Earthquake A” and “Earthquake B” are used instead of the terms “foreshock” and “main shock”, respectively. For the Aratozawa Dam, the Iwate-Miyagi Nairiku Earthquake in 2008 is considered Earthquake A in the following analysis. Before the dynamic characteristics of the dam recover, an earthquake of M_j 6.5 is modeled to occur directly underneath the dam (Earthquake B).

The acceleration records obtained at the dam base will be used directly as the input ground motions of Earthquake A. For Earthquake B, artificial seismic waves will be created with the earthquake records obtained at the dam base during the aftershocks immediately after Earthquake A. The ground motions at the dam base for Earthquake B are created by fitting the earthquake records of an aftershock equivalent to an M_j 6.5 earthquake to the lower limit spectra defined in the verification guidelines of dams during large earthquakes [4].

3.2. STUDY METHODS

The earthquake response analysis of the dam will be performed with an equivalent linearization method, which is a commonly available analysis method, instead of nonlinear analysis. The main influencing factors for the seismic behavior and seismic safety verification of dams include the ground motion, material properties such

as strength and elastic modulus, and reservoir conditions. If the material properties of the dam have changed due to Earthquake A, the variation should be reflected in the response analysis of the dam to Earthquake B. As shown in Fig. 3, the initial shear modulus and the $G/G_0-\gamma$ relationship in Period II are clearly different from those of the other periods. Therefore, to predict the earthquake responses of the dam to Earthquake B within approximately one week after Earthquake A, the initial shear modulus G_0 and the shear strain dependence of the materials during the period are considered. The residual deformation of the dam due to the doublet earthquake is

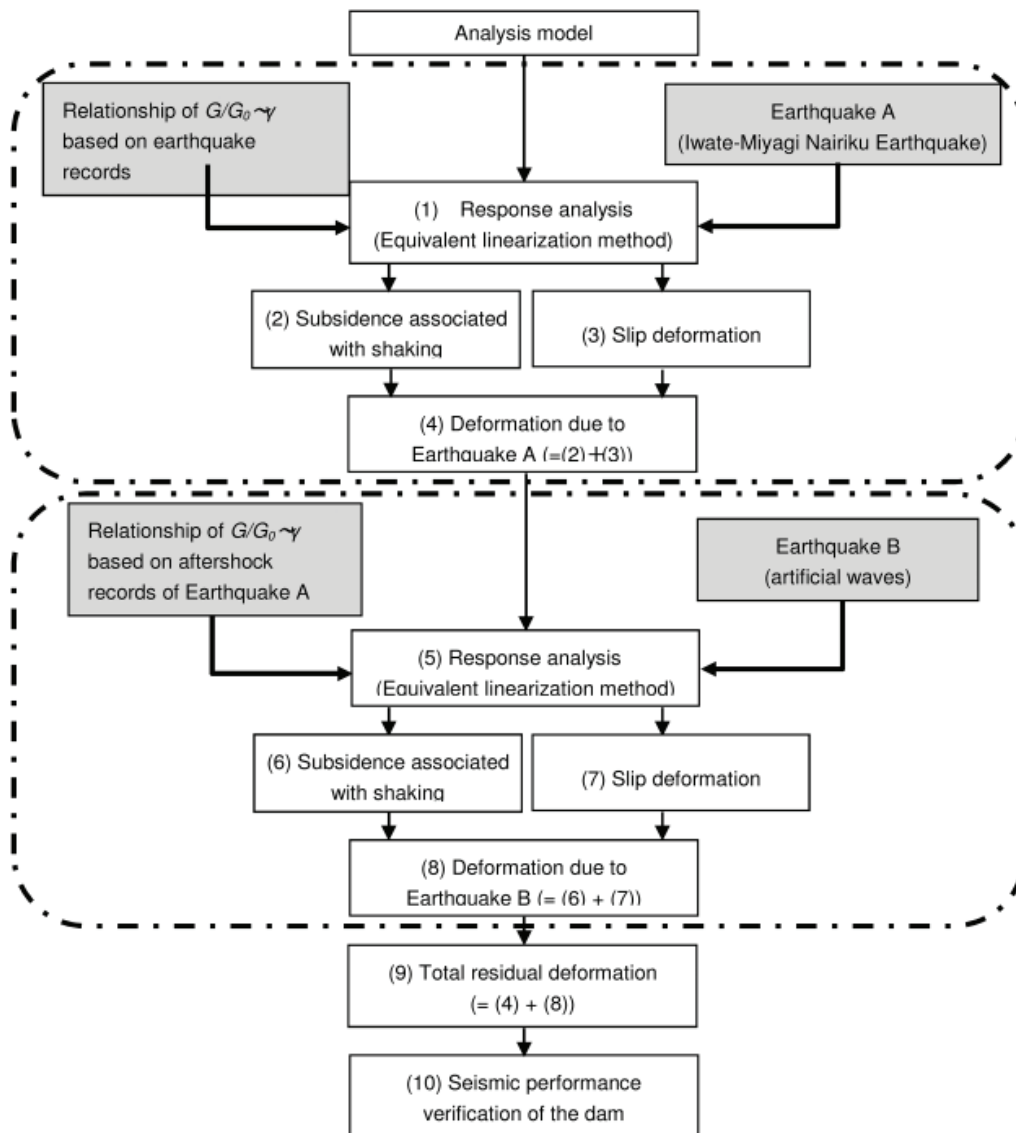


Fig. 4

Verification of the seismic performance of rockfill dams for doublet earthquakes.
Vérification de la performance sismique des barrages en enrochement pour les tremblements de terre "doublet".

predicted by summing the deformations calculated separately for each earthquake. The deformation includes the sliding component and the subsidence associated with soil particle oscillation. Figure 4 shows the earthquake response analysis and the seismic performance verification procedure for rockfill dams subject to a large doublet earthquake used in this study.

4. RESPONSE OF THE DAM TO EARTHQUAKE A

4.1. REPRODUCTION ANALYSIS

Figure 5 shows the 3D analysis model of the dam-reservoir-foundation system. Considering the influence of the vibration of the free fields outside the analysis region, viscous boundary conditions are used at the perimeter and bottom boundaries of the foundation rock and the upstream end of the reservoir model. In the static stress analysis before the earthquake, the influence of the reservoir water on the water level (EL 270.1 m) during the earthquake and that of the pore water pressure inside the dam are considered. However, the influence of the hydrodynamic pressure is neglected in the earthquake response analysis since the interaction between embankment material and reservoir water is not yet fully understood.

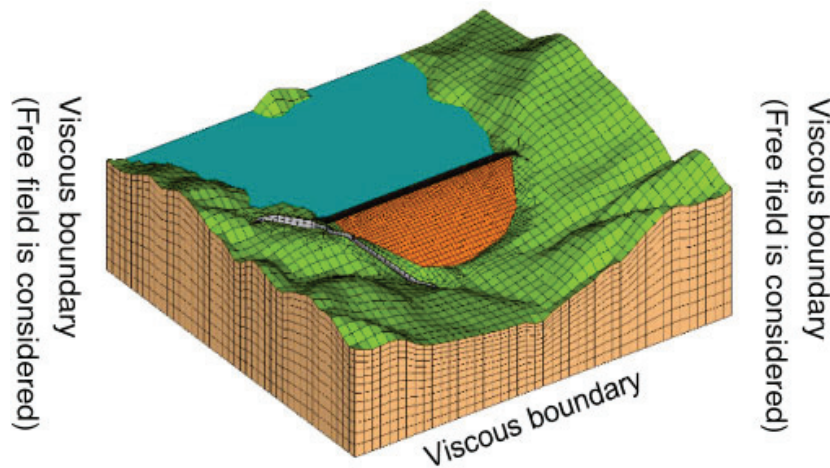


Fig. 5
Analysis model.
Modèle d'analyse.

The equivalent linearization method is used in the analysis to consider the influence of nonlinear material properties. The initial shear moduli of the embankment materials are set according to Sawada's equation [7], which is based on the

compressional and shear wave logging (P-S logging) of a number of rockfill dams. To improve the accuracy of the initial shear moduli, they are adjusted slightly so that the fundamental frequency of the dam obtained from eigenvalue analysis is consistent with the result estimated for past small earthquakes. The approximate curve in the normal status shown in Fig. 3 is used for considering the shear strain dependence of the shear moduli.

The damping is evaluated by Eq. [3] and considered to be classical Rayleigh damping.

$$[C]^e = \alpha[M]^e + \beta[K]^e \quad (3)$$

where [C], [M], and [K] are the damping matrix, mass matrix and stiffness matrix, respectively. Superscript *e* indicates that these matrices belong to each element. α and β are the parameters defined by Eq. [4].

$$\alpha = 1.4h\omega_1 \quad \beta = 0.6h/\omega_1 \quad (4)$$

where ω_1 is the fundamental angular frequency of the dam; and the damping ratio *h* is evaluated by Eq. [5], which considers its shear strain dependence.

$$h = h_{\max} \frac{\gamma}{\gamma + \gamma_r} + h_0 \quad (5)$$

where *h*, *h*₀ and *h*_{max} are the damping ratio, its initial value and its maximum value, respectively. The values of *h*₀ and *h*_{max} are listed in Table 3 and Fig. 6 are identified by the reproduction analysis of the dynamic behavior of the dam during past earthquakes [6]. γ is the effective shear strain (2/3 of its maximum value). γ_r is the reference shear strain, which can be found from Fig. 3 to be approximately 2.9×10^{-4} when $G/G_0 = 0.5$. The Poisson's ratios of the embankment materials are set according to Sawada's equation [7]. The densities of the embankment materials, foundation rock and spillway concrete from construction quality control tests of the dam are listed in Table 4.

Table 3
Damping factors identified by the reproduction analysis of dynamic behavior of the dam during past earthquakes.

Classification	Maximum damping ratio <i>h</i> _{max}	Initial damping ratio <i>h</i> ₀
A: Lower part of the core	20%	5%
B: Upper part of the core	30%	
C: Filter: Transition	30%	
E: Rock (inner): Rock (outer)	20%	

Spillway concrete is treated as a linear material with an elastic modulus of 30000 N/mm² and a Poisson's ratio of 0.2. The foundation rock is also modeled as

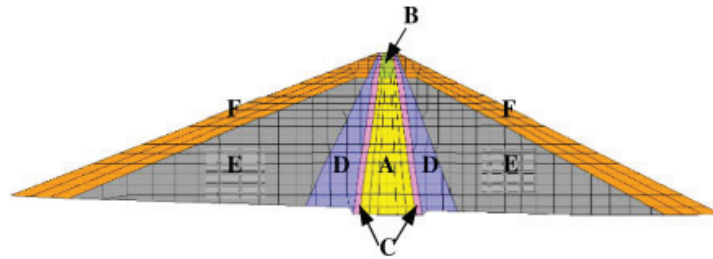


Fig. 6

Zoning of the properties (refer to Table 3).
Zonage des propriétés (se reporter au Tableau 3).

Table 4
 Density of the materials used in the analysis.

Classification	Density (g/cm ³)		
	Wet	Saturated	
Core	2.04	2.10	
Filter	2.34	2.43	
Transition	2.24	2.33	
Upstream rock	Inner	2.15	2.29
	Outer	2.15	2.32
Downstream rock	Inner	2.18	2.32
	Outer	2.13	2.30
Spillway concrete	2.40		
Bedrock	2.60		

a linear material. Its shear modulus is 5500 N/mm², which is obtained by converting from the average shear wave velocity of the rock ($V_s = 1440$ m/s). The Poisson's ratio of the foundation rock is 0.25, which is estimated to be the average value of the rock.

As for the input ground motions, since Earthquake A is a real earthquake, the earthquake records (shown by the solid line in Fig. 7(c)) obtained at the dam base (F) during the Iwate-Miyagi Nairiku Earthquake in 2008 are used. The input ground motions at the bottom boundary of the model (as shown in Fig. 5) are created by inverse analysis of the earthquake records at the dam base.

Figure 7 shows the acceleration response histories of the earthquake monitoring stations. Although there is some difference in the maximum acceleration values between the analysis results and earthquake records, the response waveforms are generally coincident. Good reproducibility is obtained in the acceleration response histories. The waveforms from 0 sec to 4 sec in the acceleration response histories of the crest have approximately the same phase. In contrast, in the waveforms after 4 sec, the peak values of the earthquake records appear slightly later than those of the analysis results. This is thought to be due to the fact that in the equivalent

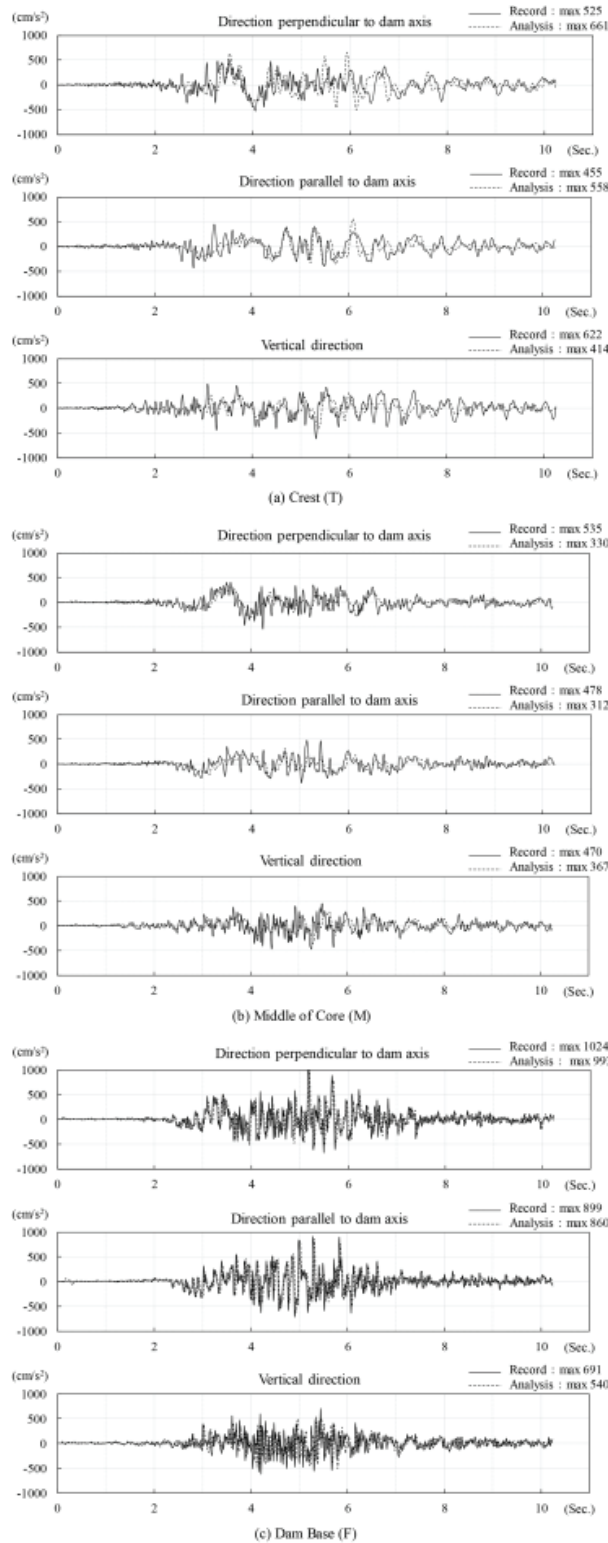


Fig. 7
 Acceleration response of Earthquake A.
 Réponse d'accélération du tremblement de terre A.

linearization method, the stiffness of the embankment materials is a constant value for the whole history, but in the actual dam, the rigidity of the dam decreased after the principal motion of the earthquake, which resulted in a decelerating wave propagation. Figure 8 shows the comparison of the Fourier spectra and the transfer

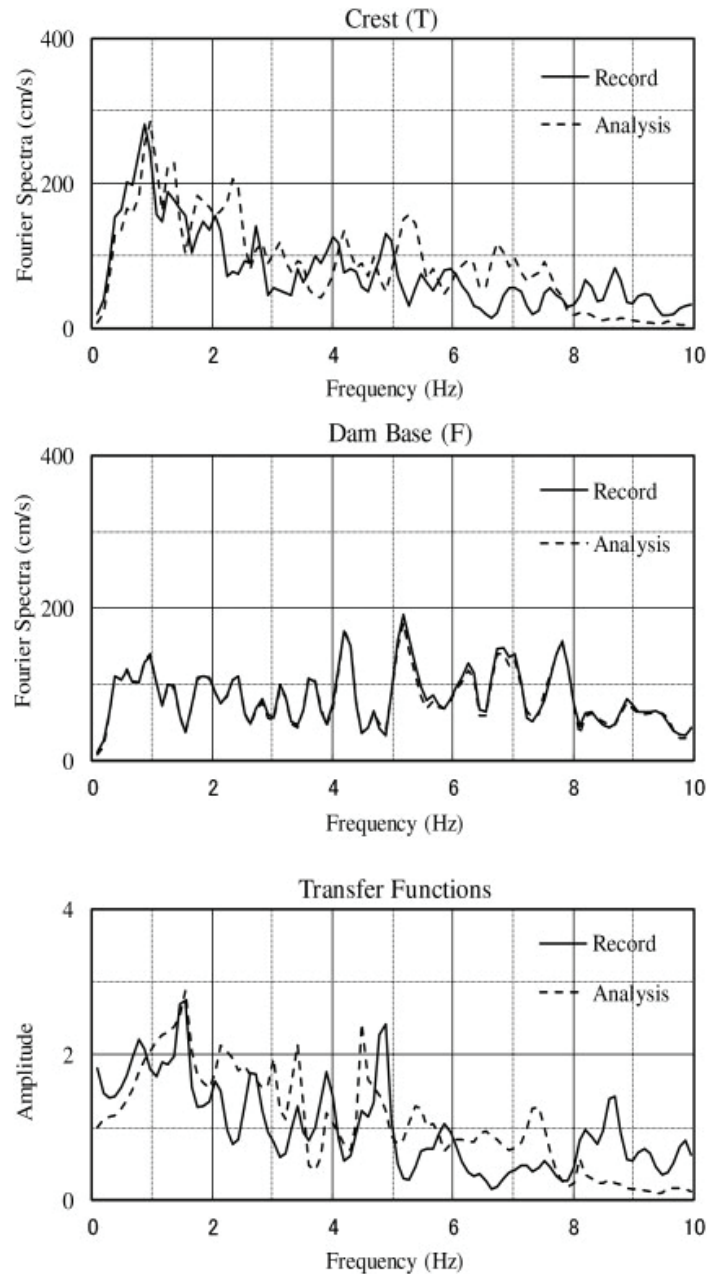


Fig. 8

Fourier spectra and transfer function of the acceleration response in the direction perpendicular to the dam axis.

Spectre de Fourier et fonction de transfert de la réponse d'accélération perpendiculairement à l'axe du barrage.

functions of the acceleration responses at the dam base and crest. In the frequency range up to 2 Hz, the Fourier spectra and transfer functions between the earthquake records and analysis results are similar. In the higher frequency range, the deviation between the analysis results and earthquake records gradually increases as the frequency increases. This finding may also be due to the continuous change in the physical properties of the real dam, while the physical properties in the analysis are treated as constant values. As a result, the physical properties suitable for the principle motion, which mainly include the low-frequency components, lead to the differences in the high-frequency seismic responses in the analysis.

4.2. RESIDUAL DEFORMATION CAUSED BY EARTHQUAKE A

The seismic performance of rockfill dams is evaluated via residual deformation under the current guidelines [4]. In the previous section, the seismic behavior of the Aratozawa Dam in response to Earthquake A was reproduced by numerical analysis. Using the analysis results, the residual deformation of the dam caused by Earthquake A is calculated. The residual deformation of the dam caused by the earthquake will be calculated separately via two methods according to the two deformation mechanisms, sliding and subsidence.

First, the deformation due to sliding is calculated. Here, the method proposed by Watanabe and Baba [8] is used, which is based on the sliding block assumption and the stress results of the earthquake response analysis. A 2D calculation is performed with the standard cross-section extracted from the 3D model shown in Fig. 5. In total, 1235 arcs are set up, covering all the possible sliding zones. To fully investigate the stability of the dam, the arcs sliding toward the upstream side are divided into 3 groups. The arcs for which both ends pass through only the upstream surface of the dam are referred to as the “U1 Group”. Those with their upper end at the crest and lower end at the upstream surface are categorized into the “U2 Group”. In addition, the arcs that cut the core zone are referred to as the “U3 Group”. Similarly, the arcs sliding downstream are divided into the “D1 Group”, “D2 Group” and “D3 Group”. Fig 9(a) shows the arcs of the U2 Group as an example. Table 5 shows the strength parameters of the embankment materials based on the results of material tests during dam construction.

As a result, except for one arc each near the upstream and downstream toes of the dam, the safety factors of all of the other arcs are greater than 1. The arc of the minimum safety factor in the 6 arc groups is summarized in Table 6, and the positions of the corresponding arcs are shown in Fig. 10. For the sliding arcs with safety factors lower than 1, the sliding displacement is calculated and shown in Table 6. In the local surface layer of the downstream slope of the dam (the No. 4 arc), the sliding safety factor is 0.847, but nearly no sliding displacement occurs (0.04 cm). This result suggests that the sliding in the Aratozawa Dam did not occur during Earthquake A (the Iwate-Miyagi Nairiku Earthquake in 2008). This result is

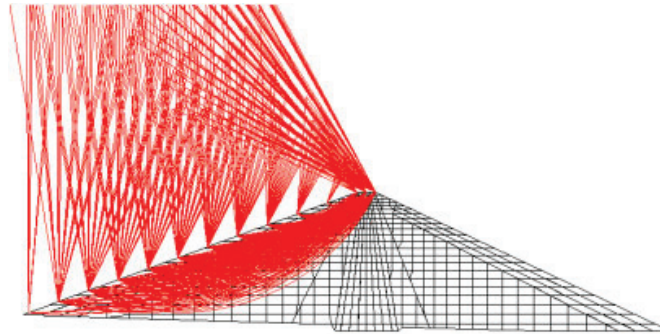


Fig. 9
Arcs of the U2 Group (as an example of sliding arcs).
Arcs du groupe U2 (comme exemple d'arcs glissants).

Table 5
Strength parameters of the embankment materials.

Division		Cohesion (MPa)	Friction angle (degrees)	Evidence
Core		0.049	33.2	Based on triaxial compression test
Filter		0.078	42.2	
Transition		0.039	39.9	
Upstream rock zone	Inner	0.049	42.7	
	Outer	0.049	43.4	
Downstream rock zone	Inner	0.049	40.2	
	Outer	0.049	42.7	

Table 6
The results of sliding deformation for Earthquake A.

Slip direction	Arc group	Arc No.	Safety factor	Slip disp. (cm)
To the upstream side	U1	1	0.994	0.0001
	U2	2	1.469	–
	U3	3	1.478	-
To the downstream side	D1	4	0.847	0.04
	D2	5	1.239	–
	D3	6	1.407	–

consistent with the field survey after the earthquake [9], which reported that no slip phenomenon was found to be due to the earthquake.

It has been noted that, in addition to sliding, subsidence may be caused by the shaking and rearrangement of the soil particles in fill dams due to strong earthquakes. Such deformation can be regarded as a result of the decrease in the rigidity of the dam. Subsidence can be conveniently evaluated by deformation calculation

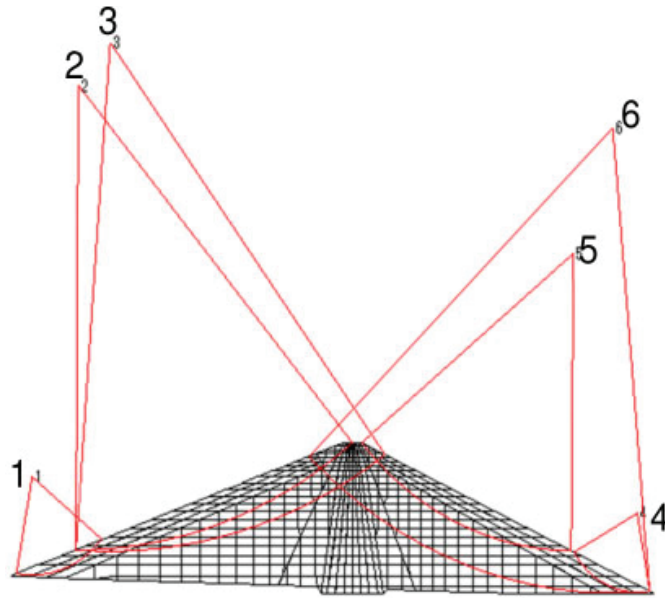


Fig. 10

Arcs with the minimum safety factor of each arc group for Earthquake A.
Arcs avec un facteur de sécurité minimum de chaque groupe d'arc pour le tremblement de terre A.

due to dead load, using the shear moduli of the embankment materials before and after the earthquake (Railway Technical Research Institute 1997). Here, the rigidities of the embankment materials before Earthquake A are evaluated by the initial shear moduli used in the earthquake response analysis, and those after the earthquake are evaluated by the converged shear moduli with the equivalent linearization method. The 3D model shown in Fig. 5 is used for this analysis. The difference in the deformation before and after the earthquake can be regarded as the residual deformation caused by the earthquake. That is,

$$U_r = U_a - U_b \quad (6)$$

where U_r is the residual deformation caused by the earthquake and U_b and U_a are the deformations due to dead load before and after the earthquake, respectively.

Figure 11 shows the deformation due to this mechanism after Earthquake A. In the standard cross-section of the dam, the maximum value of subsidence is 5.44 cm. The maximum subsidence of 5.53 cm occurs at the crest of the dam in the dam axial section.

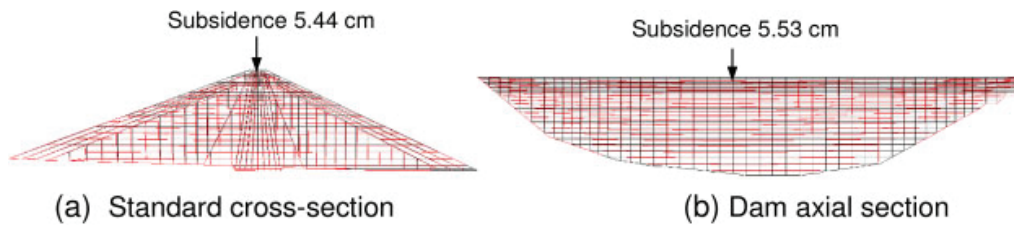


Fig. 11

Subsidence related to the shaking and rearrangement of the soil particles caused by Earthquake A.

Affaissement lié aux secousses et au réarrangement des particules du sol provoqués par le tremblement de terre A.

During an earthquake, sliding and subsidence related to the shaking and rearrangement of soil particles may occur simultaneously. However, the sliding displacement of a rigid block cannot be directly added to the calculated subsidence results. As an estimation of the possible maximum subsidence at the crest, the vertical component of the slippage at the crest can be summed with the subsidence related to the shaking and rearrangement of the soil particles. Since no sliding behavior was observed during Earthquake A, the residual deformation of the dam caused by Earthquake A equals that related to the shaking and rearrangement of soil particles, with a maximum value of 5.53 cm at the crest of the dam. According to the field survey after Earthquake A, the subsidence at the crest of the Aratozawa Dam was approximately 20 cm (Shimamoto et al. 2008). However, since the survey was conducted 16 days after the mainshock, the measured subsidence includes the contributions of many aftershocks, and other events since December 4, 2007. Therefore, the exact residual deformation caused by Earthquake A itself cannot be confirmed.

5. RESPONSE OF THE DAM TO EARTHQUAKE B

5.1. EARTHQUAKE RESPONSE ANALYSIS

Using the same model shown in Fig. 5 but with the material properties exhibited after Earthquake A, the response of the Aratozawa Dam to the Earthquake B is analyzed with the equivalent linearization method. As shown in Fig. 3, after Earthquake A, the shear moduli of the embankment materials dropped to approximately 58% of those before Earthquake A ($G/G_0 = 0.58$ corresponding to the shear strain 1.0×10^{-6}) for approximately one week. In consideration of the nonlinearity of the materials, the earthquake response analysis is performed by the equivalent linearization method using the approximate curve in the aftershock period, as shown in

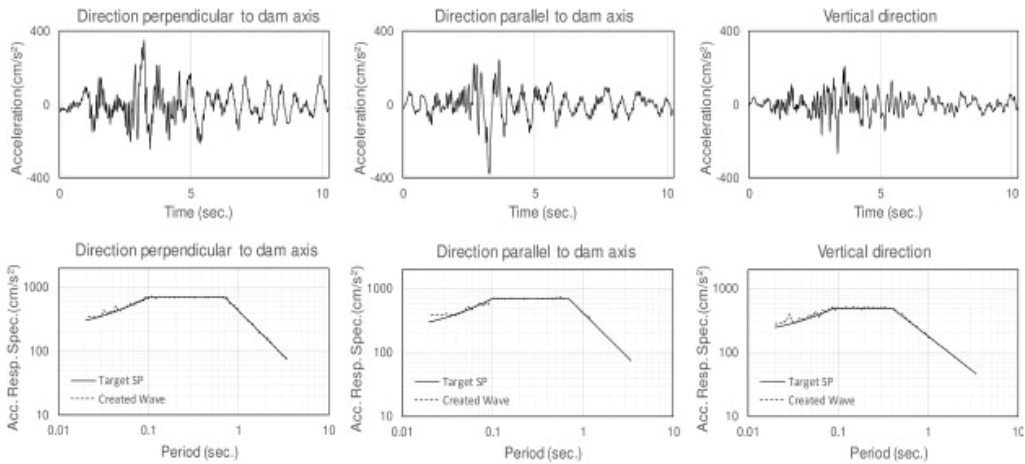


Fig. 12

Synthetic ground motion at the dam base during Earthquake B (by fitting the earthquake record of an aftershock to the lower limit response spectrum).
Mouvement synthétique du sol à la base du barrage pendant le tremblement de terre B (en ajustant l'enregistrement du tremblement de terre d'une réplique au spectre de réponse de limite inférieure).

Fig. 3. The damping is thought to increase with the decrease in the material rigidity. Because the quantitative variation is unknown, the values shown in Table 3 and Eq. [5] are used to obtain a conservative evaluation.

For setting Earthquake B, it is assumed that a potential fault exists directly under the dam, causing an M_j 6.5 earthquake. The ground motion at the dam base is created by fitting an earthquake record of a past earthquake to the lower limit response spectrum specified in the current guidelines (MLIT 2005). Here, the earthquake record at the dam base (F) in the aftershock that occurred 62 hours after the Iwate-Miyagi Nairiku Earthquake in 2008 is used. Figure 12 shows the acceleration waveforms and the spectra of the created ground motions.

5.2. RESIDUAL DEFORMATION CAUSED BY EARTHQUAKE B

As in the case of Earthquake A, the sliding deformation is calculated for the standard cross-section. The stiffness of the embankment materials was greatly reduced due to Earthquake A. Therefore, the residual strength of the embankment materials should be used in the calculation due to Earthquake B. The results of triaxial compression tests of Shichigasyuku Dam materials [10], which are similar to the materials of the Aratozawa Dam, are used here. The residual strength factors used in the slippage calculation are shown in Table 7. The calculation results are summarized in Table 8 and Fig. 13. Compared with the upstream side, the slip

Table 7
Residual strength parameters of embankment materials for the calculation of sliding deformation caused by Earthquake B.

Classification		Cohesion (MPa)	Friction angle (deg.)	Notes
Core		0.	22.1	As the residual strength parameters, cohesion is set to be zero, and frictional angle is 2/3 of the peak value.
Filter			28.1	
Transition			26.6	
Upstream rock zone	Inner		28.5	
	Outer		28.9	
Downstream rock zone	Inner		26.8	
	Outer		28.5	

Table 8
Results of sliding calculations for Earthquake B.

Sliding dir.	Group	No.	Safety factor	Max. sliding disp. (cm)	Max.subsidence (cm)
To the upstream side	U1	1	0.384	2.80	1.99
	U2	2	0.935	0.04	0.02
	U3	3	1.279	-	-
To the downstream side	D1	4	0.700	46.20	32.91
	D2	5	0.789	76.76	49.80
	D3	6	0.950	1.71	1.10

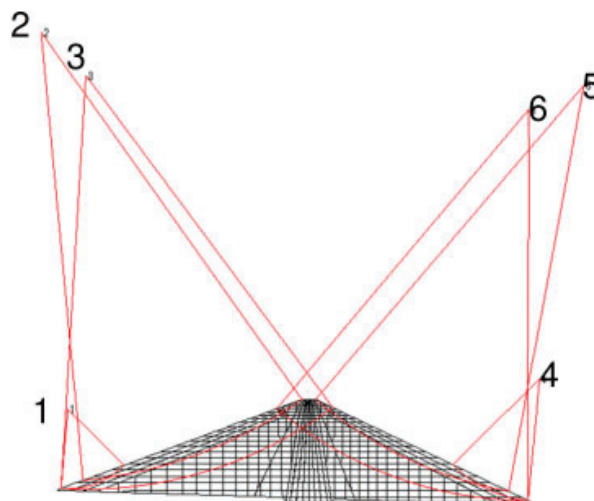


Fig. 13
The arcs with the maximum slippage in each group caused by Earthquake B.
Les arcs avec le glissement maximum dans chaque groupe provoqué par le tremblement de terre B.

displacement on the downstream side is larger overall. This is presumed to be due to the difference in the slope angle of the upstream and downstream and the strength of the materials. The slope of the upstream surface is 1:2.7, while that of the downstream surface is 1:2.1. In addition, as shown in Table 7, the frictional angles of the downstream rock zones are slightly smaller than those of the upstream side.

The sliding deformations to the upstream side are generally judged to be permissible. To the downstream side, although the sliding section of the No. 4 arc exhibits a displacement of 46.20 cm, it is very localized in the vicinity of the downstream toe. The sliding section of the No. 5 arc passes through the crest with a sliding displacement of 76.76 cm. The subsidence at the crest accompanying the sliding reaches 49.80 cm.

Figure 14 shows the residual deformation of the dam associated with the shaking and rearrangement of soil particles caused by Earthquake B. Regarding the maximum potential subsidence of the dam crest caused by Earthquake B, it is possible to sum the vertical components calculated by the above two methods. This sum is estimated to be 76.20 cm (49.80 cm + 26.40 cm) at the crest.

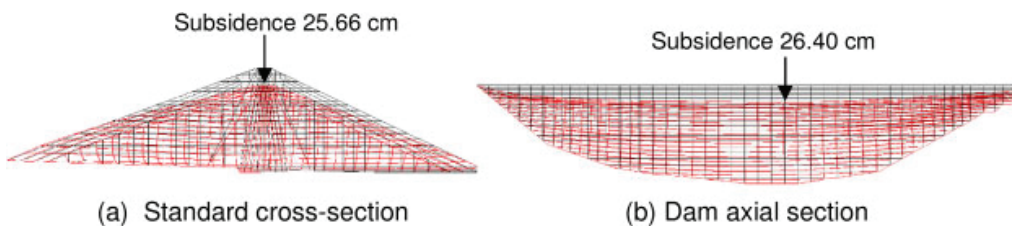


Fig. 14

Residual deformation related to the shaking and rearrangement of the soil particles caused by Earthquake B.

Déformation résiduelle liée aux secousses et au réarrangement des particules du sol provoqués par le tremblement de terre B.

5.3. RESIDUAL DEFORMATION CAUSED BY THE DOUBLET EARTHQUAKE

The deformation caused by the doublet earthquake is calculated by summing the deformation induced by Earthquake A and Earthquake B. As the maximum possible subsidence at the dam crest, the vertical components of the slip deformation and that related to the shaking and rearrangement of the soil particles can be summed directly as long as the location used for each estimate remains the same. The maximum possible subsidence at the dam crest caused by the doublet earthquake is predicted to be 81.27 cm. By comparing the subsidence calculated above with the dam freeboard (200 cm), it is considered that the earthquake may not induce

immediate overflow. However, the subsidence of the crest reaches an amount that requires detailed investigation, for example, via elastic-plastic analysis.

5.4. PROPOSAL OF EMERGENCY MEASURES AFTER A LARGE EARTHQUAKE

Even rockfill dams constructed by modern construction techniques are not likely to suffer from liquefaction due to a large earthquake, but the following events are considered to occur.

- 1) Overflow due to the excessive subsidence of the crest
- 2) Concentrated seepage along the slip surface cross the core
- 3) Water penetration through cracks
- 4) Increment of the amount of seepage flow and the generation of turbidity of seepage water

Since these phenomena may cause dam failure, emergency inspection immediately after a large earthquake is essential. As revealed in this study, there is potential risk that the seismic performance of a rockfill dam may temporarily decline due to the change in the dynamic characteristics and material properties after a large earthquake. Therefore, in preparation for a large earthquake that may occur later, it is proposed to lower the reservoir water to a safe level and keep it for a week. The counter measure is also needed to prevent the infiltration of water into the cracks. In addition, careful monitoring of the dam body and timely analysis of records are recommended.

6. CONCLUSIONS

The seismic performance verification of a rockfill dam for a large doublet earthquake was tested. A practical verification procedure was proposed.

The variation history of the material properties of the Aratozawa Dam is clarified by analyzing 19 earthquake records. The material properties of rockfill dams may change temporarily in response to strong seismic motion. If another large earthquake occurs before the dynamic characteristics of the dam and the properties of the embankment materials recover, the subsidence of the dam may increase significantly. From the viewpoint of dam safety management, it is necessary to quickly lower the reservoir water to a safe level and keep it at the lower level for at least 1 week in preparation for a large doublet earthquake.

The stiffness of the rockfill dam that experiences a strong earthquake may recover to its normal status after approximately 1 week. During this period, careful

frequent monitoring is necessary. Moreover, early remedial action to fix the damaged portion of the dam body is needed.

ACKNOWLEDGEMENTS

Many thanks to the Miyagi Prefecture Kurihara Dam Management Office and the Japan Commission on Large Dams for providing us with the earthquake records and the information about the dam used in the present study.

REFERENCES

- [1] OHMACHI T. and TAHARA T. Nonlinear earthquake response characteristics of a central clay rockfill dam, *Soils and Foundations*, Vol.51, No.2, 2011, 227–238.
- [2] MATSUMOTO N., YASUDA N., and CAO Z. Investigation on the long-term fluctuation of the dynamic characteristics and transmitting behaviors of seismic waves in a rockfill dam – foundation system, *Journal of Structural Mechanics and earthquake Engineering, JSCE*, No.74 / I-3, 2018, 319–329.
- [3] Earthquake Engineering Committee, Japan Society of Civil Engineers (JSCE). Report on the damage surveys and investigations following the 2016 Kumamoto Earthquake, Maruzen Publishing Co., Ltd., 2017 (in Japanese).
- [4] Ministry of Land, Infrastructure, Transport and Tourism (MLIT), River Bureau. Guideline for seismic performance verification of dams against large earthquakes in Japan (draft), 2005 (in Japanese).
- [5] YASUDA N. and MATSUMOTO N. Comparisons of deformation characteristics of rockfill materials using monotonic, cyclic loading and in-situ tests, *Canadian Geotechnical Journal*, Vol.31, No.2, 1994, 162–174.
- [6] YASUDA N., MATSUMOTO N., and CAO Z. Study on the Mechanism of the Peculiar Behaviors of the Aratozawa Dam During the 2008 Earthquake, *Journal of Disaster Research*, Vol.13 No.1, 2018, 205–315.
- [7] Railway Technical Research Institute. Design standards of railway structures, Maruzen Publishing Co., Ltd., 1997 (in Japanese).
- [8] SAWADA Y. and TAKAHASHI T. Study on the material properties and the earthquake behaviors of rockfill dams, 4th Japan Earthquake Engineering Symposium, 1975, 695-702 (in Japanese).

- [9] WATANABE H and BABA K. A Study of sliding stability evaluation method based on the dynamic analysis of fill dams, *Large Dam*, No.97, 1981, 25–38.
- [10] SHIMAMOTO K., SATO N., OMACHI T., et al. Report on damage to dams caused by the 2008 Iwate/Miyagi inland earthquake, 2008.
- [11] HOJO K., HARITA K. and OGAWA M. Large-scale tri-axial test for the characteristics of filldam materials, Technical memorandum of PWRI, No.1507, Public Works Research Institute, Ministry of Construction, 1979.